The Factor IXa Heparin-Binding Exosite Is a Cofactor Interactive Site: Mechanism for Antithrombin-Independent Inhibition of Intrinsic Tenase by Heparin†

Qiu-Ping Yuan, Erik N. Walke, and John P. Sheehan*

Department of Medicine/Hematology, University of Wisconsin−Madison, Madison, Wisconsin 53706

Received September 23, 2004; Revised Manuscript Received December 18, 2004

ABSTRACT: Therapeutic heparin concentrations selectively inhibit the intrinsic tenase complex in an antithrombin-independent manner. To define the molecular target and mechanism for this inhibition, recombinant human factor IXa with alanine substituted for solvent-exposed basic residues (H92, R170, R233, K241) in the protease domain was characterized with regard to enzymatic activity, heparin affinity, and inhibition by low molecular weight heparin (LMWH). These mutations only had modest effects on chromogenic substrate hydrolysis and the kinetics of factor X activation by factor IXa. Likewise, factor IXa H92A and K241A showed factor IXa−factor VIIIa affinity similar to factor IXa wild type (WT). In contrast, factor IXa R170A demonstrated a 4-fold increase in apparent factor IXa−factor VIIIa affinity and dramatically increased coagulant activity relative to factor IXa WT. Factor IXa R233A demonstrated a 2.5-fold decrease in cofactor affinity and reduced ability to stabilize cofactor half-life relative to wild type, suggesting that interaction with the factor VIIIa A2 domain was disrupted. Markedly (R233A) or moderately (H92A, R170A, K241A) reduced binding to immobilized LMWH was observed for the mutant proteases. Solution competition demonstrated that the EC_{50} for LMWH was increased less than 2-fold for factor IXa H92A and K241A but over 3.5-fold for factor IXa R170A, indicating that relative heparin affinity was WT > H92A/K241A > R170A ≫ R233A. Kinetic analysis of intrinsic tenase inhibition demonstrated that relative affinity for LMWH was WT > K241A > H92A > R170A ≫ R233A, correlating with heparin affinity. Thus, LMWH inhibits intrinsic tenase by interacting with the heparin-binding exosite in the factor IXa protease domain, which disrupts interaction with the factor VIIIa A2 domain.

In vitro and ex vivo modeling of coagulation demonstrates that activation of factor Xa by the intrinsic tenase complex (factor IXa−factor VIIIa) is the rate-limiting step for thrombin generation during the propagation phase of coagulation (*1*−*5*). The essential in vivo role of the intrinsic tenase complex is emphasized by the hemophilia A and B phenotypes. The rate-limiting step for thrombin generation is also likely to be important for expression of clinical thrombotic phenotypes. In particular, the majority of established risk factors for venous thrombosis (decreased antithrombin, protein C, and protein S; elevated factors VIII, IX, and XI; factor V Leiden and prothrombin 20210A) predominantly affect the propagation, as opposed to the initiation, phase of coagulation (*6*−*12*). The critical role of the intrinsic tenase complex in propagation of the coagulation response makes it an attractive target for the development of specific antithrombotic agents (*1*, *2*, *5*). Treatment with active site-blocked factor IXai or monoclonal antibody versus the factor IX Gla domain is as effective as unfractionated or low molecular weight heparin in animal models of thrombosis and demonstrates significantly less bleeding risk at equivalent therapeutic doses (*13*−*17*). These animal models suggest that selective inhibition of factor IX(a), in the presence of intact tissue factor-induced coagulation, may reduce the bleeding complications of antithrombotic therapy. Targeting the factor IXa active site is problematic due to the poor reactivity of this protease with peptide substrates and inhibitors, which reflects the partially collapsed nature of the active site observed in crystal structures (*18*, *19*). However, defining relevant cofactor or substrate binding exosite(s) on factor IXa will identify novel molecular targets for inhibition of the intrinsic tenase complex.

The precise mechanism for the antithrombotic efficacy of heparin is incompletely understood but can be inferred from treatment of human thrombotic disorders. Low molecular weight heparin (LMWH)[1] and unfractionated heparin are equally efficacious for the treatment of venous thromboembolism (*20*−*22*). This therapeutic equivalence suggests that a template mechanism, requiring chains greater than 16−18 oligosaccharides long, is not critical to the clinical efficacy of heparin. Conformational activation of antithrombin by heparin pentasaccharide stimulates the inhibition of both factor IXa and factor Xa through exosite-mediated interactions; however, assembly of these proteases into membrane-bound enzyme complexes results in relative protection from

† This research was supported by a Grant-in-Aid from the Northland Affiliate of the American Heart Association and a grant from the Wisconsin Alumni Research Foundation (J.P.S.).

* Address correspondence to this author. Phone: (608) 262-1964. Fax: (608) 263-4969. E-mail: jps@medicine.wisc.edu.

[1] Abbreviations: APTT, activated partial thromboplastin time; BSA, bovine serum albumin; DME, Dulbecco's modified Eagle's media; Gla, γ-carboxyglutamic acid; HEPES, *N*-(2-hydroxyethyl)piperazine-*N*′-2-ethanesulfonic acid; LMWH, low molecular weight heparin; PC−PS, phosphatidylcholine−phosphatidylserine; PEG-8000, poly(ethylene glycol) (average molecular weight 8000); PL, phospholipid.

10.1021/bi047934a CCC: $30.25
Published on Web 02/10/2005

inhibition (*23*−*26*). In contrast, therapeutic concentrations of unfractionated, low molecular weight, or low-affinity (for antithrombin) heparin inhibit the intact intrinsic tenase complex in an antithrombin-independent manner. This inhibition is selective for the intrinsic tenase complex, as neither the prothrombinase nor the tissue factor−factor VIIa complexes are inhibited in this manner (*27*). The relative contribution of antithrombin-dependent and -independent mechanisms to the antithrombotic efficacy of heparin is undefined. However, antithrombin-independent mechanisms have demonstrated in vivo antithrombotic efficacy, suggesting a potential contribution to the therapeutic effects of heparin (*28*).

Phosphorothioate oligonucleotides are polyanionic polymers that inhibit factor X activation by the intrinsic tenase complex via interaction with an exosite on factor IXa (*29*, *30*). Similarly, heparin oligosaccharides inhibit factor X activation by intrinsic tenase through direct binding to a factor IXa exosite, which disrupts a critical protease−cofactor interaction (*31*). Defining the relevant exosite(s) on factor IXa will identify novel molecular targets for therapeutic inhibition of the intrinsic tenase complex. To define the molecular target for antithrombin-independent inhibition by heparin, and the role of this exosite in regulating enzymatic activity of the intrinsic tenase complex, we have mutated solvent-exposed basic residues located in the putative heparin-binding exosite of full-length factor IXa. The recombinant factor IXa proteins were characterized to determine the contribution of this exosite to assembly and enzymatic activity of the intrinsic tenase complex, heparin affinity, and inhibition of factor X activation by LMWH. The results indicate that the heparin-binding exosite of factor IXa is the molecular target for antithrombin-independent inhibition of the intrinsic tenase complex by heparin and represents a cofactor interactive site for the factor VIIIa A2 domain.

EXPERIMENTAL PROCEDURES

Materials. Human plasma-derived factor X, factor XIa, and thrombin were purchased from Enzyme Research (South Bend, IN). Recombinant human factor VIII (Kogenate FS) was generously provided by Andreas Mueller-Beckhaus of the Bayer Corp. (Berkeley, CA). Recombinant hirudin, bovine serum albumin, and poly(L-lysine) were purchased from Sigma (St. Louis, MO). Chromogenic substrates were purchased as follows: S-2765 (*N*-α-benzyloxycarbonyl-D-Arg-Gly-Arg-pNA) from DiaPharma (Franklin, OH) and Pefachrome IXa (CH_3SO_2-D-CHG-Gly-Arg-pNA) from Centerchem, Inc. (Stamford, CT). LMWH (dalteparin) was obtained from Pharmacia and UpJohn Co. (Kalamazoo, MI). Biotinylated LMWH (ardeparin) was purchased from Celsus, Inc. (Cinncinati, OH). GelCode Blue and biotin-X-hydrazide were obtained from Pierce Endogen (Rockford, IL). Strepavidin-coated surface plasmon resonance sensor chips were purchased from BiaCore, Inc. (Piscataway, NJ). Phosphatidylserine (PS) and phosphatidylcholine (PC) were purchased from Avanti Lipids (Alabaster, AL). Cholesterol was purchased from Calbiochem (San Diego, CA). Phosphatidylcholine−phosphatidlylserine−cholesterol (molar ratio 75:25:1) phospholipid vesicles (PC−PS vesicles) were prepared by extrusion through a 100 nm polycarbonate filter (*32*). The molar concentration of phospholipid was determined with an elemental phosphorus assay (*33*). Geneticin (G418) was purchased from Gibco-BRL (Gaithersburg, MD). Sheep anti-human factor IX (PAHIX-G) was from Haematologic Technologies Inc. (Burlington, VT), and monoclonal alkaline phosphatase conjugated anti-goat/sheep IgG clone GT-34 was from Sigma (St. Louis, MO).

Mutagenesis and Expression of Recombinant Human Factor IX. pCMV5 vector containing the human factor IX cDNA (pCMV5-FIX) was generously provided by Darrel Stafford (University of North Carolina). Alanine substitutions were introduced into the factor IX sequence by PCR-based mutagenesis using the QuickChange site-directed mutagenesis kit (Stratagene, La Jolla, CA). The constructs FIX-H92A, FIX-R233A, and FIX-K241A (amino acid residues identified by chymotrypsin numbering) were generated using the wild-type pCMV5-FIX plasmid as a template, and constructs were confirmed by full-length sequencing of the cDNA. Human embryo kidney (HEK) 293 cell lines stably transfected with the cDNA for factor IX wild type and factor IX R170A were also provided by Darrel Stafford (*34*). Additional HEK 293 cells were cotransfected with mutant pCMV5-FIX (10 μg) and pSV2neo (1 μg) plasmids by calcium phosphate precipitation. Stably transfected cell lines for each mutant construct were selected by limiting dilution in the presence of 0.5 mg/mL Genetecin (*35*). Resistant clones expressing the highest levels of recombinant FIX were selected by Western blotting of serum-free media supernatant with polyclonal anti-human FIX antisera. Wild-type and selected mutant factor IX cell lines were expanded in T-175 cm^2 flasks (Corning Life Sciences, Corning, NY) with 50% DME/50% Ham's F12 media containing 10% fetal bovine serum. Upon reaching confluency, cell layers were rinsed three times with PBS and incubated in serum-free medium containing 10 μg/mL vitamin K and insulin−transferrin−selenite media supplement (Sigma, St. Louis, MO). The conditioned medium was harvested every 48 h for 10 days and centrifuged to remove cellular debris, and 5 mM benzamidine was added prior to storage at −80 °C.

Purification and Activation of Recombinant FIX. Upon thawing, the conditioned media was filtered, applied to a Q-Sepharose column (35 mL) equilibrated in 0.15 M NaCl and 20 mM HEPES, pH 7.4, at 2 mL/min, and washed with at least 10 column volumes of buffer. Recombinant factor IX was eluted with a 0.15−1.0 M NaCl gradient in 20 mM HEPES, pH 7.4, at 1 mL/min. The major peak was pooled and dialyzed overnight versus 0.15 M NaCl and 20 mM HEPES, pH 7.4. This pool was then filtered and applied to a Mono Q HR 5/5 column equilibrated with the same buffer at 1 mL/min. After being washed for at least 10 column volumes, human FIX was eluted with a calcium chloride gradient (0−45 mM), and the first peak (representing fully γ-carboxylated protein) was pooled, dialyzed overnight, and frozen in aliquots at −80 °C (*36*, *37*). Protein concentrations were initially determined by absorbance at 280 nm using an extinction coefficiency ($\epsilon_{0.1\%}$) of 1.43. Purified factor IX was activated with human factor XIa (150:1 substrate:enzyme molar ratio) at 4 °C for 2−6 h depending on the mutant protein. Complete or nearly complete (>95%) activation of factor IXa was documented by SDS−PAGE, and factor XIa was depleted by incubation with polyclonal anti-human factor XI antisera cross-linked to Affi-Gel beads in a spin column. The Abs_{280} of the purified factor IXa was determined, and

the protein was placed in aliquots at −80 °C. An aliquot was later thawed to quantitate factor IXa catalytic sites by titration with antithrombin III (ATIII) as described (*38*), except that the factor IXa−antithrombin−heparin incubation step was prolonged (60 min) to ensure the reaction was complete for recombinant factor IXa with decreased heparin affinity. The active protease concentration determined by antithrombin titration was used for enzymatic and binding analyses of the recombinant proteins.

Chromogenic Substrate Hydrolysis and Plasma Coagulant Activity of the Recombinant Factor IXa. The rate of hydrolysis of Pefachrome IXa was determined at room temperature in a reaction containing final concentrations of 100 nM recombinant factor IXa in tenase buffer (0.15 M NaCl, 20 mM HEPES, pH 7.4, 2 mM $CaCl_2$, 1 mg/mL BSA, 0.1% PEG-8000), 30% ethylene glycol, and 125−500 μM Pefachrome IXa. Initial rates of substrate cleavage were determined by monitoring the absorbance at 405 nm over 10 min in a kinetic microtiter plate reader (V_{max} Reader, Molecular Devices Corp.). The catalytic efficiency (k_{cat}/K_M) of each recombinant factor IXa for Pefachrome IXa was determined from the slope of substrate concentration versus the initial rate of substrate cleavage (moles per minute), using a path length of 0.53 cm for the 150 μL volume and a molar extinction coefficient of 9920 M^{-1} cm^{-1} for *p*-nitroaniline. Coagulant activity was determined in an activated partial thromboplastin time (APTT) with addition of recombinant factor IXa to factor IX-deficient plasma just prior to recalcification. Clotting times were determined in a Start 4 coagulometer, and relative activity of the recombinant proteins was determined by comparison to a standard curve constructed by serial dilution of pooled normal plasma into factor IX-deficient plasma (George King Bio-Medical, Overland Park, KS).

Factor X Activation by the Factor IXa−Phospholipid and Factor IXa−Factor VIIIa Complexes. Factor X activation was determined by chromogenic assay as previously described (*31*). Factor X activation by factor IXa−phospholipid in the absence of cofactor was determined over 20 min at room temperature in a reaction containing 5 nM recombinant human factor IXa, 50−750 nM factor X, 50 μM PC−PS vesicles, and 30% ethylene glycol in tenase buffer. Factor X activation by the factor IXa−factor VIIIa−phospholipid complex was determined in a reaction containing 0.1 nM recombinant human factor IXa, 1.0 or 2.0 nM thrombin-activated factor VIIIa, and 50 μM PC−PS phospholipid vesicles in tenase buffer. The reaction was initiated by addition of factor X immediately after factor VIIIa and incubated for 15−30 s for determination of factor X kinetics (or 60 s for other assays) at room temperature. The reaction was terminated by addition of EDTA/polybrene, and the amount of factor Xa was determined by comparing the rate of S-2765 substrate hydrolysis to a standard curve as described (*31*). Incubation times were restricted to conditions under which less than 10% total substrate cleavage occurred. Kinetic constants for factor X activation were obtained by plotting the rate of factor Xa generation (nanomolar per minute) versus substrate concentration and fitting the data by nonlinear regression to the Michaelis−Menten equation.

Determination of the Affinity (Apparent K_D) for Factor VIIIa−Factor IXa Complex Formation. The affinity of the factor IXa_B−factor VIIIa complex was assessed by monitoring intrinsic tenase complex activity at limited concentrations of FVIIIa as described (*31*). Thrombin-activated factor VIIIa (0.15 nM) was incubated with increasing amounts of factor IXa (0−15 nM), in the presence of 50 μM PC−PS, and 200 nM factor X. Factor IXa concentration was plotted versus the rate of factor Xa generation, and the data were fit by nonlinear regression to a single site binding model to determine the $K_{D(app)}$. The factor IXa−factor VIIIa concentration for each recombinant factor IXa under assay conditions was calculated using the experimentally determined $K_{D(app)}$ to solve the quadratic equation as described (*31*).

Determination of the in Vitro Half-Life of Factor VIIIa. The in vitro half-life of factor VIIIa activity was determined for cofactor alone, cofactor plus PC−PS vesicles, and cofactor plus PC−PS vesicles and factor IXa. Recombinant factor VIII (20 nM) was activated with 40 nM thrombin for 30 s and neutralized with 60 nM hirudin, followed by a 1:2 dilution into buffer alone, buffer plus 100 μM PC−PS vesicles, or buffer plus 100 μM PC−PS vesicles and 40−80 recombinant factor IXa. Aliquots were removed from the factor VIIIa incubation mixtures over time and diluted 25-fold into the intrinsic tenase assay containing 1.5 nM factor IXa and 200 nM factor X to determine residual factor VIIIa activity. Starting activity was normalized to 100%, activity was plotted versus time, and the data were fit to an exponential function (*27*). Alternatively, the in vitro half-life of the intrinsic tenase complex in the absence and presence of 2 μM LMWH was determined in a reaction containing 1.0 nM thrombin-activated factor VIIIa, 0.2 nM factor IXa, and 50 μM PC−PS vesicles in tenase buffer, by varying the time of factor X (200 nM) addition between 0 and 15 min.

Equilibrium Binding Analysis of Factor IXa−LMWH Affinity Using Surface Plasmon Resonance. Flow cells for the reference surface and immobilized LMWH binding surface on a BiaCore SA chip were prepared as described (*31*). Briefly, a reference surface was created by injecting 20 μL of 8 μM biotin-X-hydrazide (Pierce Endogen) at 10 μL/min in 0.3 M NaCl, 20 mM HEPES, pH 7.4, and 0.05% Tween-20 (cell 1). A high-capacity LMWH surface was similarly created by injecting 20 μL of 200 μg/mL biotin−low molecular weight heparin (ardeparin) at 10 μL/min, resulting in an ∼350 RU signal (cell 2). Binding surfaces were regenerated with 1 M NaCl and 20 mM HEPES, pH 7.4. Direct binding of recombinant proteins to the immobilized LMWH surface was assessed by injection of 250 nM factor IXa at 5 μL/min for 120 s (association phase) followed by 2 μM LMWH at 5 μL/min for 180 s (dissociation phase). Final sensorgrams were obtained by subtracting the reference surface from the LMWH surface signal, averaging replicate determinations, and subtracting the mean sham injection (buffer only) signal (*39*).

To further characterize the relative affinity of selected recombinant factor IXa mutants for LMWH, a competition binding assay was performed to determine the EC_{50} for soluble LMWH. Recombinant factor IXa (100 nM) was incubated with increasing concentrations of LMWH (0.01−100 μM) for 10 min at room temperature prior to injection at 5 μL/min for 120 s. For each LMWH concentration, the final sensorgram response at 90 s postinjection was plotted as the relative proportion of remaining free factor IXa, with the response units for FIXa alone (no LMWH) normalized

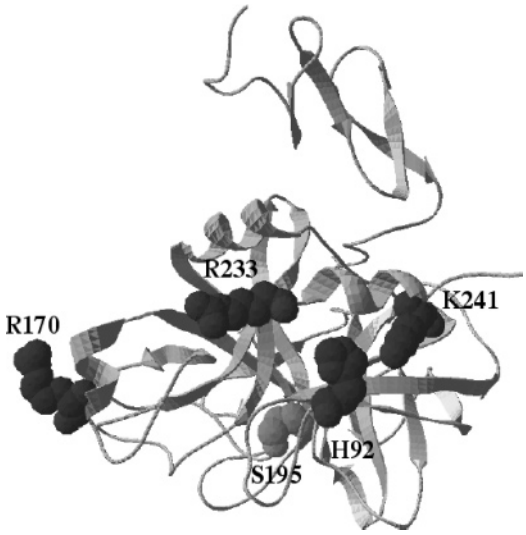

FIGURE 1: Representation of the crystal structure of human factor IXa EGF2−protease fragment. The crystal structure of the factor IXa−EGF fragment (1RFN) is represented by a ribbon diagram created with SwissPdb-viewer. The EGF2 domain is positioned on top of the protease domain, with the active site oriented downward. The active site Ser195 (light gray) and surface residues mutated to alanine (dark gray) are labeled and highlighted with a space-filling representation of their respective side chains.

to 1. The EC_{50} was determined by fitting the data to the equation:

$$B = \frac{(EC_{50})^n}{(EC_{50})^n + [I]^n} \quad (1)$$

where B represents the fractional specific binding, [I] represents the concentration of LMWH used as competitor, EC_{50} represents the concentration of LMWH that causes a 50% reduction in the surface plasmon binding response, and n represents the pseudo Hill coefficient (*40*).

Determination of the K_I for Inhibition of Factor X Activation by LMWH. The rate of factor X activation by the intrinsic complex in the presence of LMWH was determined over 60 s at room temperature in a reaction containing 1.0 nM FVIIIa, 0.2 nM recombinant FIXa, 200 nM FX, and 50 μM PC−PS. The rate of factor X generation was plotted versus LMWH concentration, and the data were fit by nonlinear regression to the equation for partial noncompetitive inhibition to determine the values for $V_{max(app)}$, $V(i)_{max(app)}$, and K_I for LMWH (*27*, *30*, *41*, *42*). $V_{max(app)}$ and $V(i)_{max(app)}$ represent the maximal velocity in the absence and presence of inhibitor, and K_I is the dissociation constant for the enzyme−inhibitor complex.

RESULTS

Expression, Activation, and Active Site Titration of Recombinant Factor IXa. The putative heparin-binding exosite on human factor IXa was targeted by substituting alanine for basic surface residues (Figure 1) in a protease region homologous to previously identified heparin-binding sites on thrombin and factor Xa (*43*, *44*). Targeted residues included H92 (chymotrypsin numbering), located at the base of the c91−101 insertion loop, R170A in the c165−170 α-helix known to participate in cofactor binding, and R233 and K241A in the C-terminal α-helix. Recombinant factor IX proteins expressed in HEK 293 cells were purified to homogeneity from conditioned media and analyzed by 4−20% gradient SDS−PAGE. All of the recombinant FIX proteins demonstrated high purity by Coomassie Blue staining, with a single band of approximately 55000 Da under nonreducing conditions (Figure 2). Recombinant factor IX proteins were activated to factor IXa by incubation with human factor XIa and titrated with antithrombin in the presence of unfractionated heparin to determine the number of active sites present (see Experimental Procedures). Systematic variation of the incubation time for factor IXa−antithrombin demonstrated that titrations were essentially complete by 60 min, even for factor IXa mutants with reduced heparin affinity (see below).

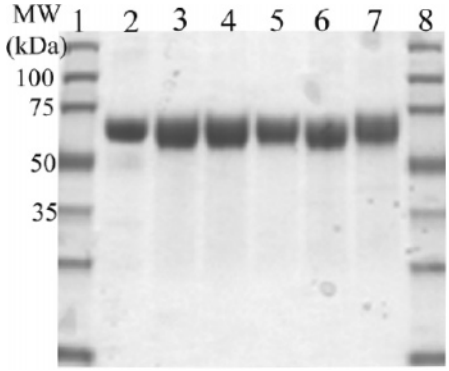

FIGURE 2: 4−20% SDS−PAGE analysis of the purified recombinant factor IX. The purified recombinant factor IX proteins (1.5 μg/well) were loaded onto a 4−20% gradient gel, subjected to SDS−PAGE under nonreducing conditions, and stained with GelCode Blue (Pierce Scientific). Lanes: 1 and 8, molecular weight standards; 2, plasma-derived factor IX; 3−7, recombinant factor IX wild type, H92A, R170A, R233A, and K241A, respectively.

Chromogenic Substrate Cleavage and Coagulant Activity of Recombinant Factor IXa. The ability of active site-titrated recombinant factor IXa to cleave the chromogenic substrate Pefachrome IXa (CH_3SO_2-D-CHG-Gly-Arg-pNA) was examined in the presence of 30% ethylene glycol (*45*). The initial rate of substrate cleavage at 125−500 μM Pefachrome IXa was determined to establish the specificity constant (k_{cat}/K_M) of each recombinant factor IXa for the peptide substrate. Recombinant factor IXa wild type, H92A, R233A, and K241A all demonstrated a similar k_{cat}/K_M for Pefachrome IXa to plasma-derived factor IXa (data not shown), suggesting that the active site and S1−S3/4 subsites of these proteases were intact. Factor IXa R170A demonstrated an approximately 1.5-fold increase in catalytic efficiency (k_{cat}/K_M ratio) for the peptidyl substrate relative to wild-type factor IXa (Table 1), suggesting that this mutation may have a distant effect on the protease active site or a more proximal effect on the S1−S3/4 subsites. The coagulant activity of the recombinant factor IXa was determined by APTT in factor IX-deficient plasma. Similar to previous results, factor IXa R170A had significantly increased coagulant activity relative to wild-type factor IXa (372%) (*34*). Factor IXa H92A (89%) demonstrated a modest decrease in coagulant activity relative to the wild-type protein, while factor IXa R233A (59%) and K241A (64%) demonstrated moderate reductions in coagulant activity (Table 1).

Effect of Factor IXa Mutations on Apparent Factor IXa−Factor VIIIa Affinity. The effect of alanine substitutions in the putative heparin-binding exosite of factor IXa on interac-

Table 1: Enzymatic and Coagulant Activity of Recombinant Factor IXa[a]

enzyme (FIXa)	Pefachrome IX k_{cat}/K_m ($mM^{-1}s^{-1}$)	clotting activity (%)	FIXa−FVIIIa affinity $K_{D(app)}$ (nM)	factor X (FIXa−PL) k_{cat}/K_m ($M^{-1}s^{-1}$)	factor X (FIXa−FVIIIa−PL) k_{cat}/K_m ($M^{-1}s^{-1}$)
WT	0.75	100	1.7	8.1×10^3	1.6×10^8
H92A	0.75	89	1.9	10.0×10^3	1.4×10^8
R170A	1.18	372	0.4	9.1×10^3	1.2×10^8
R233A	0.79	59	4.4	5.8×10^3	1.5×10^8
K241A	0.81	64	2.2	8.6×10^3	2.0×10^8

[a] The initial rate of Pefachrome IX cleavage (125−500 μM) by 100 nM factor IXa and the kinetics of factor X (25−750 nM) activation by 5 nM factor IXa with 50 μM PC−PS vesicles present were determined in tenase buffer (0.15 M NaCl, 20 mM HEPES, pH 7.4, 2 mM $CaCl_2$, 1 mg/mL BSA, 0.1% PEG-8000) with 30% ethylene glycol present. Coagulant activity was determined by APTT in factor IX deficient plasma. The apparent affinity of the factor IXa−factor VIIIa complex was determined by titration of 0.15 nM factor VIIIa with factor IXa (0−15 nM) in the presence of 200 nM factor X and fitting the data to a single site binding model. The kinetics of factor X activation (0−125 nM) by the intrinsic tenase complex (0.1 nM factor IXa, 1.0 nM factor VIIIa, 50 μM PC−PS) were determined in tenase buffer. Factor VIIIa concentration was increased to 2.0 nM for factor IXa R233A in these assays, due to lower cofactor affinity. The k_{cat} for factor X activation was calculated by dividing the $V_{max(app)}$ by the predicted factor IXa−factor VIIIa concentration based on the experimentally determined $K_{D(app)}$ (see Experimental Procedures).

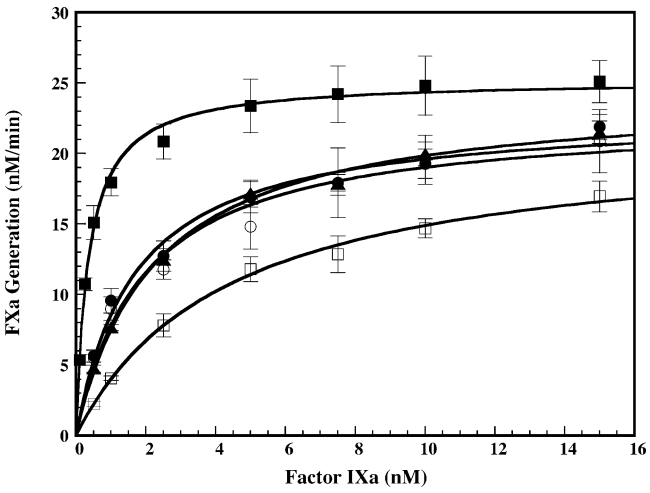

FIGURE 3: Effect of factor IXa mutations on the affinity of the factor IXa−factor VIIIa complex on PC−PS vesicles. The apparent affinity ($K_{D(app)}$) of the factor IXa−factor VIIIa interaction was determined using enzymatic activity to detect complex formation. The rate of factor X activation by factor IXa−factor VIIIa was determined by adding increasing concentrations of factor IXa (0−15 nM) into a reaction containing 0.15 nM factor VIIIa, 200 nM factor X, and 50 μM PC−PS vesicles. Mean values were plotted versus factor IXa concentration with error bars representing ±SD ($n = 4$). The $K_{D(app)}$ was determined by fitting the data to a single site binding model. The $K_{D(app)}$ and B_{max} values ± SE for the recombinant factor IXa proteins were as follows: wild type (●), 1.7 ± 0.3 nM and 22.9 ± 1.0 nM/min; H92A (○), 1.9 ± 0.4 nM and 22.7 ± 1.3 nM/min; R170A (■), 0.4 ± 0.03 nM and 25.2 ± 0.3 nM/min; R233A (□), 4.4 ± 0.4 nM and 21.4 ± 0.8 nM/min; and K241A (▲), 2.2 ± 0.2 nM and 24.3 ± 0.6 nM/min, respectively.

tion with cofactor was assessed by kinetic determination of factor IXa−factor VIIIa affinity (Figure 3). Factor IXa wild type, H92A, and K241A demonstrated similar affinity for activated cofactor, suggesting that these mutations did not disrupt the factor IXa−factor VIIIa interaction on PC−PS

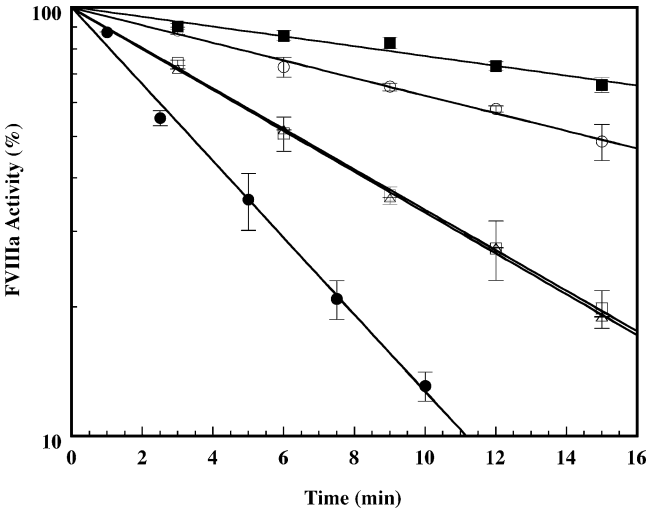

FIGURE 4: Effect of factor IXa mutations on the ability to stabilize the in vitro half-life of factor VIIIa. Recombinant factor VIII was activated for 30 s with 40 nM thrombin, neturalized with 60 nM hirudin, and immediately diluted 1:2 into the tenase reaction buffer in the absence or presence of 50 μM PC−PS vesicles and 20−40 nM factor IXa. Residual factor VIIIa activity was determined by sampling into the intrinsic tenase assay as described (see Experimental Procedures), and the data were fit to a simple exponential decay. Mean values for factor VIIIa activity were plotted versus time with error bars representing ±SD ($n = 3$). The time course of cofactor activity is shown for factor VIIIa alone (●); factor VIIIa, 50 μM PC−PS, and 20 nM factor IXa wild type (○), R170A (■), and R233A (□); or 40 nM factor IXa R233A (△). The k_{obs} for loss of factor VIIIa activity was 0.21 min^{-1} for cofactor alone, 0.05 min^{-1} for 20 nM factor IXa wild type plus phospholipid, 0.03 min^{-1} for 20 nM factor IXa R170A plus phospholipid, and 0.11 min^{-1} for 20 or 40 nM factor IXa R233A plus phospholipid.

vesicles. In contrast, the $K_{D(app)}$ of factor IXa R233A for cofactor was increased 2.5-fold compared to wild type, suggesting that this mutation disrupts an important interactive site for factor VIIIa (Figure 3). This reduction in cofactor affinity is consistent with the reduced coagulant activity of this protein (Table 1). In contrast to a previous report (*34*), the $K_{D(app)}$ of factor IXa R170A for factor VIIIa was decreased over 4-fold relative to wild type, suggesting that this mutation significantly increases the affinity for cofactor and providing an explanation for the increased coagulant activity of this protein. The c165−170 insertion loop has previously been implicated in cofactor binding by site-directed mutagenesis and analysis of type II hemophilia B mutations (*46*−*48*). Modification of cofactor affinity by the mutations R170A and R233A suggests that these residues may contribute to an extended factor VIIIa interactive site.

Effect of Factor IXa Mutations on the Ability of Factor IXa To Stabilize the in Vitro Half-Life of Factor VIIIa. The cofactor activity of factor VIIIa degrades in first-order manner due to the loss of the noncovalently associated A2 domain (*49*). The in vitro half-life of factor VIIIa is significantly prolonged in the presence of factor IXa and phospholipid vesicles (*50*). To further assess the effect of the R170A and R233A mutations on the factor VIIIa interaction, the ability to stabilize cofactor activity was compared for factor IXa wild type, R170A, and R233A (Figure 4). Addition of 20 nM factor IXa wild type or R170A prolonged the in vitro half-life of factor VIIIa relative to cofactor alone or cofactor plus phospholipid vesicles (not shown), with a 4- or 7-fold reduction in the rate constant

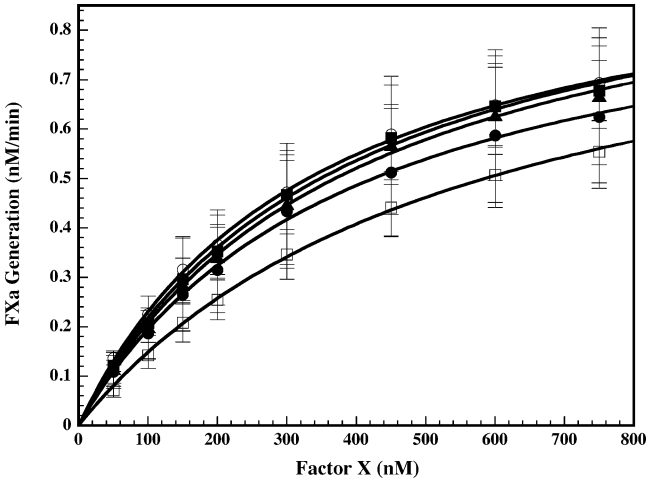

FIGURE 5: Effect of factor IXa mutations on the kinetics of factor X activation by factor IXa−phospholipid in the presence of 30% ethylene glycol. The rate of factor X activation by factor IXa was determined in reactions containing 5 nM factor IXa, 25−750 nM factor X, and 50 μM PC−PS vesicles in 0.15 M NaCl, 20 mM HEPES, pH 7.4, 2 mM $CaCl_2$, 1 mg/mL BSA, 0.1% PEG-8000, and 30% ethylene glycol. Mean values were plotted with error bars representing ±SD ($n = 4$). The $K_{m(app)}$ and $V_{max(app)}$ for factor X activation were determined by fitting the data by nonlinear regression to the Michaelis−Menten equation. The $K_{m(app)}$ and $V_{max(app)}$ ± SE for the recombinant factor IXa proteins were as follows: wild type (●), 395.0 ± 23.9 nM and 0.96 ± 0.03 nM/min; H92A (○), 341.3 ± 14.5 nM and 1.02 ± 0.02 nM/min; R170A (■), 379.6 ± 23.9 nM and 1.04 ± 0.03 nM/min; R233A (□), 561.3 ± 27.0 nM and 0.98 ± 0.03 nM/min; and K241A (▲), 401.6 ± 23.4 nM and 1.04 ± 0.03 nM/min, respectively.

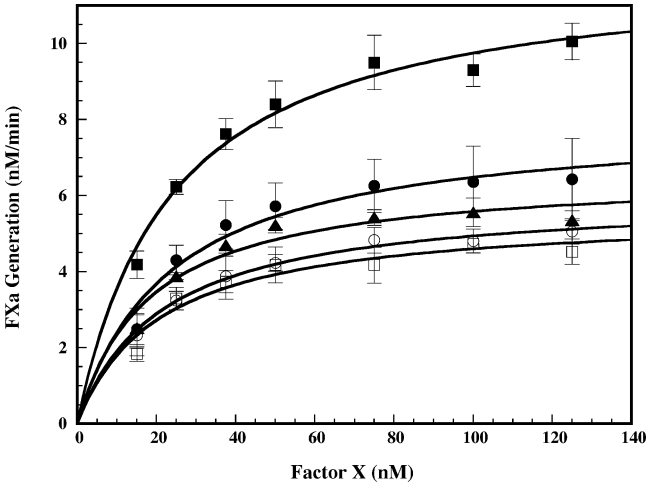

FIGURE 6: Effect of factor IXa mutations on the kinetics of factor X activation by the factor IXa−factor VIIIa−phospholipid complex. The rate of factor X activation by each recombinant factor IXa was determined in reactions containing 1.0 nM factor VIIIa, 0.1 nM factor IXa, 15−125 nM factor X, and 50 μM PC−PS in 0.15 M NaCl, 20 mM HEPES, pH 7.4, 2 mM $CaCl_2$, 1 mg/mL BSA, and 0.1% PEG-8000. Factor VIIIa concentration was increased to 2 nM for factor IXa R233A due to the significantly lower factor IXa−factor VIIIa affinity of this mutant (see Figure 3). Mean values were plotted with error bars representing ±SD ($n = 4$). The $K_{m(app)}$ and $V_{max(app)}$ for factor X activation were determined by fitting the data by nonlinear regression to the Michaelis−Menten equation. The $K_{m(app)}$ and $V_{max(app)}$ values ± SE for factor X activation by the recombinant factor IXa proteins were as follows: wild type (●), 23.5 ± 5.1 nM and 8.0 ± 0.5 nM/min; H92A (○), 21.6 ± 2.0 nM and 6.0 ± 0.2 nM/min; R170A (■), 24.0 ± 3.3 nM and 12.1 ± 0.5 nM/min; R233A (□), 20.8 ± 5.3 nM and 5.6 ± 0.4 nM/min; and K241A (▲), 18.1 ± 4.3 nM and 6.6 ± 0.4 nM/min, respectively.

for A2 dissociation, respectively. Addition of 20 nM factor IXa R233A also prolonged the factor VIIIa half-life but demonstrated only a 2-fold reduction in the rate constant. Increasing factor IXa R233A to 40 nM had no further effect on the rate constant, suggesting that the defect in the ability to stabilize cofactor activity was not simply a result of decreased factor IXa−factor VIIIa affinity. The rate of intrinsic tenase decay was also examined by varying the time of factor X addition to preformed factor IXa−factor VIIIa−phospholipid (1.0 nM factor VIIIa, 0.1 nM factor IXa) in the intrinsic tenase assay. Factor IXa R233A demonstrated a significantly more rapid decrement in the rate of factor Xa generation over time compared to factor IXa wild type (data not shown). These results suggest that the R233A mutation disrupts the interaction of factor IXa with the A2 domain of factor VIIIa.

Effect of Factor IXa Mutations on the Kinetics of Factor X Activation in the Presence and Absence of Factor VIIIa. The effect of these alanine substitutions on the kinetics of factor X activation by factor IXa−phospholipid or factor IXa−factor VIIIa−phospholipid was assessed in the presence of varying substrate concentrations. In the absence of cofactor, analysis of factor X kinetics under conditions consistent with the rapid equilibrium assumption (i.e., substrate ≫ enzyme concentration) is problematic due to the poor catalytic activity of factor IXa−phospholipid. Thus, 30% ethylene glycol was added to the buffer to accelerate factor X activation by factor IXa under these conditions (*30*, *45*). The kinetics of factor X activation by factor IXa H92A, R170A, and K241A were similar to that of the wild-type protein (Figure 5), with comparable specificity constants (k_{cat}/K_M) (Table 1). The catalytic efficiency of factor IXa R233A was modestly reduced relative to wild-type factor IXa, mostly due to an increased $K_{M(app)}$ for factor X (Figure 5).

Likewise, the kinetics of factor X activation was examined for each recombinant protease in the intrinsic tenase complex. Due to the significantly decreased cofactor affinity of factor IXa R233A, the factor VIIIa concentration was increased for this protease to ensure adequate activity for analysis of factor X kinetics. In the presence of cofactor, the apparent substrate affinity ($K_{M(app)}$) for each of the mutant factor IXa proteins was essentially unchanged relative to wild-type factor IXa (Figure 6). The $V_{max(app)}$ varied in proportion to the apparent affinity of the factor IXa−factor VIIIa complex for each mutant, as expected on the basis of the predicted effective enzyme concentration (factor IXa−factor VIIIa complex). The catalytic rate (k_{cat}) of factor X activation by factor IXa for each recombinant protein was calculated from the predicted factor IXa−factor VIIIa complex concentration on the basis of the apparent affinity ($K_{D(app)}$) determinations. All of the recombinant factor IXa mutants demonstrated a specificity constant for factor X similar to that of wild-type factor IXa under these conditions (Table 1). Thus, these mutations did not appear to drastically disrupt recognition and catalysis of factor X by factor IXa on phospholipid vesicles.

Effect of Factor IXa Mutations on the Affinity for LMWH. The effect of these alanine substitutions on the affinity of factor IXa for LMWH was assessed by a surface plasmon resonance approach (*31*). Biotinylated LMWH was immobilized on a BiaCore strepavidin sensor chip and compared to a reference cell prepared with biotin-X-hydrazide.

The relative heparin affinity of each recombinant protein was assessed by comparing the binding response after injection of 250 nM factor IXa over the immobilized LMWH surface. Factor IXa H92A, R170A, and K241A demonstrated a moderately reduced binding response to the LMWH surface relative to wild-type factor IXa, suggesting that these proteins had reduced heparin affinity. Remarkably, factor IXa R233A demonstrated minimal binding to the LMWH surface under these conditions, suggesting a marked decrease in heparin affinity for this protease (Figure 7A). To further evaluate the relative heparin affinity of factor IXa H92A, R170A, and K241A, a competition solution affinity approach was employed. Increasing concentrations of soluble LMWH were incubated with 100 nM factor IXa for 10 min prior to injection over the sensor chip. The remaining free factor IXa was detected by the residual binding response at each concentration of LMWH and plotted to determine the EC_{50} by fitting the data to eq 1 (see Experimental Procedures). Factor IXa H92A and K241A demonstrated modest increases (less than 2-fold) in the EC_{50} relative to wild type, suggesting only small reductions in heparin affinity for these proteases (Figure 7B). Factor IXa R170A demonstrated greater than a 3.5-fold increase in the EC_{50} for LMWH compared to wild type, suggesting a significantly larger decrease in heparin affinity. Factor IXa R233A could not be subjected to the competition binding analysis due to its minimal binding to the immobilized LMWH surface. Summarizing the direct and competition binding responses for LMWH suggests that the relative heparin affinity of the recombinant factor IXa proteins can be ranked as follows: wild type > H92A/K241A > R170A ≫ R233A (Figure 7).

Effect of Factor IXa Mutations on the Ability of LMWH To Inhibit Factor X Activation by the Intrinsic Tenase Complex. The effect of these mutations on the ability of LMWH to inhibit factor X activation by the intrinsic tenase complex was assessed for each recombinant factor IXa (Figure 8). Factor X activation by wild-type factor IXa was partially inhibited (~90%) similar to plasma-derived factor IXa (not shown), and fitting the data to the equation for partial, noncompetitive inhibition yielded a similar apparent inhibitor affinity (K_I). Factor IXa H92A and K241A demonstrated modest increases in the K_I for LMWH relative to wild-type factor IXa, consistent with the modest effect of these mutations on the EC_{50} for LMWH in the competition solution affinity analysis. Factor IXa R170A demonstrated significant resistance to inhibition with a 6-fold increase in the K_I for LMWH and approximately 3-fold increase in residual activity at maximal inhibition compared to the wild-type protein. Remarkably, factor IXa R233A demonstrated almost complete resistance to the inhibition of factor X activation by LMWH. Thus, the apparent inhibitor affinity of LMWH (K_I) for the intrinsic tenase complex can be ranked as follows: wild type > H92A > K241A > R170A ≫ R233A. The effect of the R233A mutation on factor IXa−factor VIIIa affinity (Figure 3), stabilization of cofactor half-life by factor IXa (Figure 4), and the rate of intrinsic tenase decay (data not shown) suggests that binding sites for the cofactor A2 domain and LMWH overlap on the factor IXa protease domain. Thus, the effect of 2 μM LMWH on the rate of intrinsic tenase decay was examined by varying the time of factor X addition to a tenase reaction containing 1.0 nM factor VIIIa and 0.2 nM factor IXa. Addition of LMWH increased the rate of intrinsic tenase decay over 2-fold, consistent with destabilization or disruption of the A2−factor IXa interaction (Figure 9).

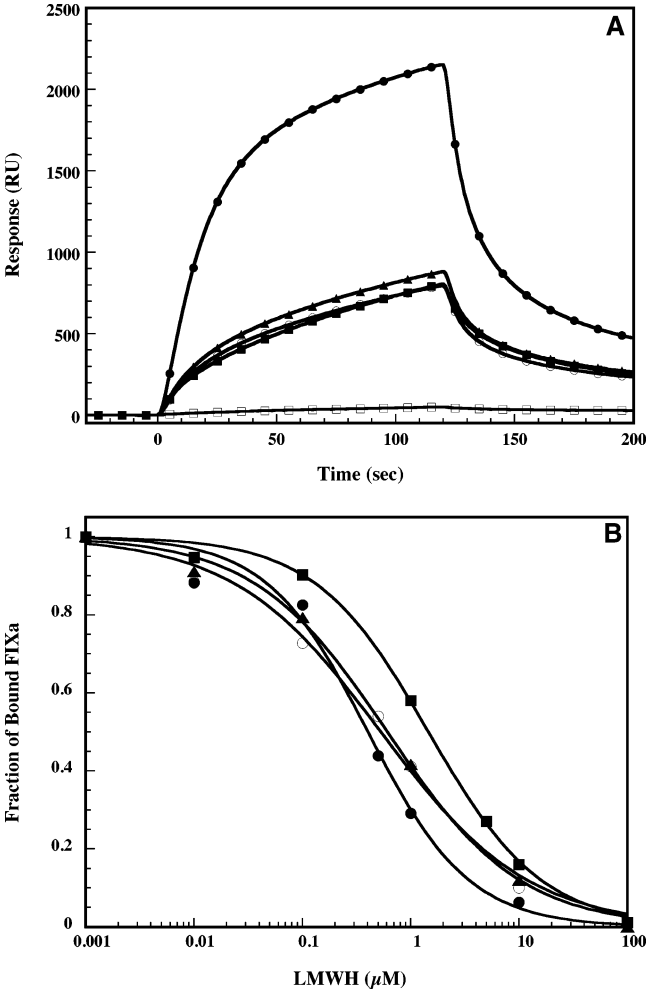

FIGURE 7: Effect of mutations on the affinity of recombinant factor IXa for LMWH. The affinity of the recombinant factor IXa for LMWH was assessed by surface plasmon resonance, analyzing direct (A) and competition (B) binding responses on an immobilized LMWH surface as described in Experimental Procedures. (A) Recombinant factor IXa (250 nM) wild type (●), H92A (○), R170A (■), R233A (□), and K241A (▲) were injected over reference and immobilized LMWH surfaces at 5 μL/min in 0.15 M NaCl, 20 mM HEPES, pH 7.4, 2 mM $CaCl_2$, and 0.05% Tween-20 surfactant for a 120 s association phase, followed by buffer with 2 μM LMWH for a 180 s dissociation phase. Final sensogram responses for each of the recombinant proteins were obtained by subtraction of the reference surface and sham (buffer only) responses from the LMWH surface response. (B) Competition solution affinity of LMWH for recombinant factor IXa. Increasing concentrations of LMWH were preincubated for 10 min with 100 nM factor IXa wild type (●), H92A (○), R170A (■), or K241A (▲) prior to injection over reference and immobilized LMWH surfaces on the BiaCore 2000. Factor IXa R233A could not be analyzed due to its extremely low baseline signal. The concentration of free factor IXa was determined by the binding response at 90 s after injection, with comparison to a standard curve (0−250 nM factor IXa) generated under identical conditions. The concentration of LMWH was plotted versus the proportion of remaining free factor IXa and fit by nonlinear regression to obtain the EC_{50} for competition by low molecular weight heparin. Each point represents the average of duplicate sensorgrams. The EC_{50} values of LMWH for recombinant factor IXa wild type, H92A, R170A, and K241A were 0.40 ± 0.05 μM, 0.64 ± 0.06 μM, 1.46 ± 0.10 μM, and 0.61 ± 0.06 μM, respectively.

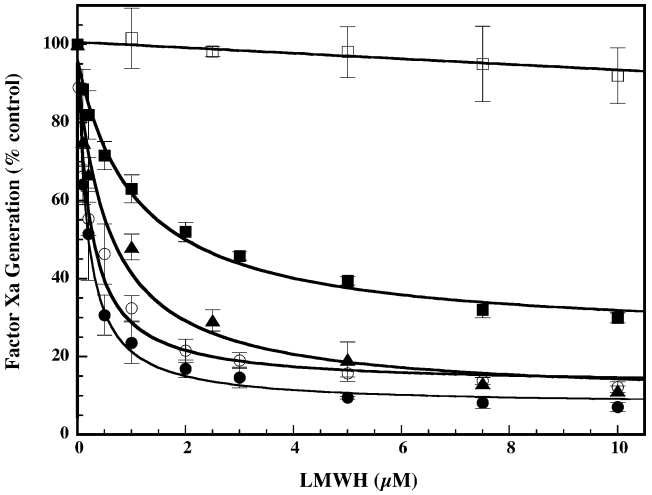

FIGURE 8: Effect of factor IXa mutations on the ability of LMWH to inhibit factor X activation by the intrinsic tenase complex. Increasing concentrations of LMWH were added to a reaction mixture containing 0.2 nM wild type (●), H92A (○), R170A (■), R233A (□), or K241A (▲) factor IXa with 1.0 nM factor VIIIa, 200 nM factor X, and 50 μM PC−PS vesicles in 0.15 M NaCl, 20 mM HEPES, pH 7.4, 2 mM $CaCl_2$, 1 mg/mL BSA, and 0.1% PEG-8000. The rate of factor X activation (nM/min) by the intrinsic tenase complex was determined in a chromogenic assay as described in Experimental Procedures. Mean values (% control, no LMWH) were plotted with error bars representing ±SD (n = 4). The inhibition constant (K_I) for LMWH was determined by fitting the data by nonlinear regression to the equation for partial, noncompetitive inhibition. The K_I values ± SE for the recombinant proteins were as follows: wild type, 0.18 ± 0.01 μM; H92A, 0.62 ± 0.23 μM; R170A, 1.08 ± 0.18 μM; R233A, >10 μM; and K241A, 0.24 ± 0.04 μM.

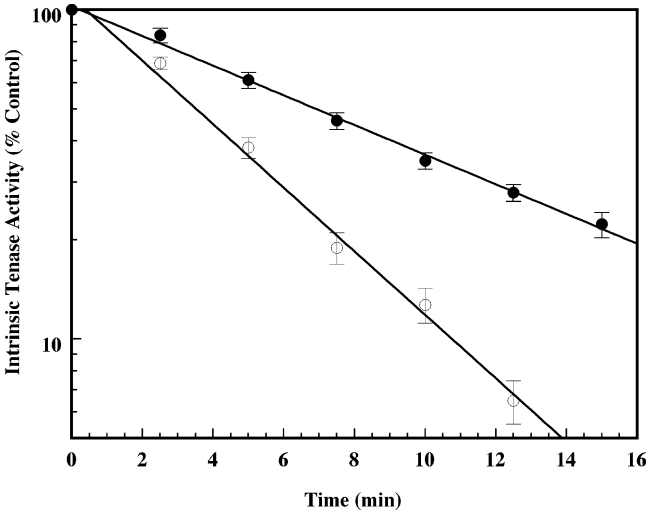

FIGURE 9: Effect of LMWH on the rate of intrinsic tenase decay. Factor X (200 nM) was added at intervals between 15 s (time 0) and 15 min after cofactor addition to 0.2 nM factor IXa wild type, 1.0 nM factor VIIIa, 50 μM PC−PS vesicles, 0.15 M NaCl, 20 mM HEPES, pH 7.4, 2 mM $CaCl_2$, 1 mg/mL BSA, and 0.1% PEG-8000 in the absence (●) or presence (○) of 2 μM LMWH. The rate of factor X activation (nM/min) by the intrinsic tenase complex was determined in a chromogenic assay as described in Experimental Procedures. Mean values (% control) were plotted with error bars representing ±SD (n = 3). The k_{obs} for intrinsic tenase decay was 0.10 and 0.22 min^{-1} in the absence and presence of 2 μM LMWH, respectively.

DISCUSSION

The putative heparin-binding exosite on full-length factor IXa was targeted by site-directed mutagenesis to investigate its role in the enzymatic activity of the intrinsic tenase complex and antithrombin-independent inhibition of factor X activation by heparin. Alanine substitutions were introduced into basic surface residues (H92, R170, R233, and K241) in a region of the factor IXa protease domain homologous to previously identified heparin-binding sites on thrombin and factor Xa (*43*, *44*). The recombinant factor IX proteins exhibited indistinguishable chromatographic behavior during calcium elution from anion-exchange resin and were purified to homogeneity as demonstrated by SDS−PAGE analysis (Figure 2). Recombinant factor IXa was activated by human factor XIa and titrated with antithrombin for enzymatic studies. Characterization of active site-titrated recombinant factor IXa demonstrated intact catalytic activity for small peptidyl substrate (Pefachrome IXa) for factor IXa H92A, R233A, and K241A relative to factor IXa wild type and modestly increased activity for factor IXa R170A (Table 1). The reason for the increase in catalytic efficiency is unknown but may involve effects of the cofactor-interactive c165−170 α-helix on conformation of the active site or S4/S3−S1 subsites of factor IXa. The coagulant activities of factor IXa H92A (89%), R233A (59%), and K241A (64%) were modestly to moderately decreased relative to wild-type factor IXa (Table 1). In contrast, factor IXa R170A had markedly increased coagulant activity (372%), consistent with previous work (*34*).

These mutations had varied effects on the apparent cofactor affinity of recombinant factor IXa, as determined in a functional binding assay. Factor IXa H92A and K241A demonstrated an affinity ($K_{D(app)}$) similar to that of wild-type factor IXa for factor VIIIa, suggesting that these mutations did not significantly affect the factor IXa−factor VIIIa interaction. Factor IXa R233A demonstrated significantly lower affinity for factor VIIIa (Figure 3), and reduced ability to stabilize cofactor half-life (Figure 4), relative to wild-type factor IXa. These results suggest that this mutation significantly disrupts the interaction with cofactor and provide a basis for the moderate reduction in coagulant activity (Table 1). At subnanomolar protease concentrations, decay of intrinsic tenase activity primarily depends on the rate of A2 domain dissociation, while at 10-fold higher protease concentrations, proteolysis of factor VIIIa dominates the rate of decay (*51*). Under the former conditions, factor IXa R233A demonstrates accelerated decay in intrinsic tenase activity relative to factor IXa wild type (data not shown), suggesting that the mutation disrupts interaction(s) between factor IXa and the A2 domain of factor VIIIa. Modeling of the factor IXa−factor VIIIa interaction suggests that the A2 domain interacts with the c165−170 α-helix but also predicts multiple contacts within the putative heparin-binding exosite (*48*). The c165−170 α-helix is involved in a cluster of type II hemophilia B mutations, and site-directed mutagenesis has clearly demonstrated it to be a cofactor interactive site (*46*−*48*, *52*). Factor IXa R233A now provides direct evidence that the cofactor interface with the A2 domain extends into the core of the heparin-binding exosite. In contrast, factor IXa R170A showed over a 4-fold increase in factor IXa−factor VIIIa affinity and increased ability to stabilize cofactor activity relative to wild-type factor IXa. The significantly higher affinity of factor IXa R170A contrasts with previous results that reported only a modest difference in cofactor affinity for this protease relative to wild-type factor IXa (*34*).

The reason for this discrepancy is unclear and may relate to specific assay conditions. However, the increased affinity of factor IXa R170A for factor VIIIa provides a basis for the remarkable coagulant activity (372%) of this protease. The specific mechanism for the increased cofactor affinity of factor IXa R170A is unclear but may involve removal of an unfavorable charge−charge interaction with factor VIIIa, as clustered basic residues in residues 484−510 of the A2 domain contribute to cofactor activity (*53*). In summary, our analysis provides direct evidence that the interaction of protease with the factor VIIIa A2 domain extends from the c165−170 α-helix to the proximal portion of the C-terminal α-helix.

In contrast, these mutations had limited effects on macromolecular substrate (factor X) catalysis by factor IXa on phospholipid vesicles in the absence or presence of factor VIIIa. The kinetics of factor X activation by factor IXa in the presence of 30% ethylene glycol was similar to that of the wild-type protein for all mutants except factor IXa R233A, which demonstrated an ∼50% increase in $K_{m(app)}$ (Figure 5). In the presence of factor VIIIa, none of these mutations had a significant effect on the apparent affinity ($K_{m(app)}$) of the enzyme complex for factor X (Figure 6). However, factor IXa R233A required an increased factor VIIIa concentration for adequate analysis due to reduced cofactor affinity. The $V_{max(app)}$ for factor X activation largely reflected the relative amount of factor IXa−factor VIIIa complex formation expected under these conditions. Using the experimentally determined $K_{D(app)}$ to calculate the effective enzyme concentration (factor IXa−factor VIIIa complex) under assay conditions, the $V_{max(app)}$ was divided by enzyme concentration to obtain the k_{cat} and catalytic efficiency (k_{cat}/K_M) for factor X activation by each recombinant factor IXa. All of the factor IXa mutants demonstrated similar catalytic efficiency (k_{cat}/K_M) to wild-type factor IXa in the presence of factor VIIIa (Table 1). Although effects on the factor IXa−factor X interaction may be obscured by the contribution of the phospholipid membrane to apparent substrate affinity (*54*, *55*), the similar catalytic efficiency of the recombinant proteins suggests that the major effect of these mutations is limited to the factor IXa−factor VIIIa interaction.

The relative affinity of recombinant factor IXa for heparin was assessed by direct and competition binding to immobilized LMWH with surface plasmon resonance detection. Factor IXa R233A exhibited minimal binding to immobilized LMWH under these conditions, indicating a profound decrease in heparin affinity (Figure 7A). Factor IXa H92A, R170A, and K241A demonstrated moderately reduced binding compared to wild-type factor IXa (Figure 7A), which was further ranked by the relative EC_{50} of soluble LMWH for each of these mutants (Figure 7B). On the basis of this analysis, the relative affinity of recombinant factor IXa for LMWH was WT > H92A/K241A > R170 ≫ R233. These observations agree well with the effect of alanine substitutions on the relative heparin affinity of Gla-domainless factor IXa (*56*). Both sets of data suggest that the major binding site for heparin is restricted to the predominant electropositive field on the protease domain, which is located between the c165−170 α-helix and the proximal portion of the C-terminal α-helix of the protease (data not shown). Additional basic residues in the C-terminal α-helix (K239, K241) that lie outside of this region contribute only modestly to apparent heparin affinity, and the binding site does not extend toward the active site, or surfaces known to participate in extended substrate binding on homologous proteases. Importantly, the effect of these mutations on the relative affinity of factor IXa for heparin correlated with the ability of LMWH to inhibit factor X activation by the intrinsic tenase complex. On the basis of apparent inhibitor affinity (K_I), the rank order for sensitivity to inhibition by LMWH was WT > K241A > H92A > R170A ≫ R233A (Figure 8). Remarkably, factor IXa R233A in the intrinsic tenase complex was almost completely resistant to inhibition of factor X activation by LMWH. The correlation between the relative heparin affinity of the protease and the ability of LMWH to inhibit factor X activation by the intrinsic tenase complex definitively demonstrates that the heparin-binding exosite on factor IXa is the molecular target for antithrombin-independent inhibition of the intrinsic tenase complex. Previous analysis of the mechanism for anithrombin-independent inhibition of intrinsic tenase suggested that heparin oligosaccharides disrupt a critical cofactor interaction with a protease exosite (*31*). These mutagenesis results now demonstrate that the heparin-binding exosite overlaps extensively with an interactive site for the factor VIIIa A2 domain on the factor IXa protease domain. These results are consistent with the contribution of the factor Xa heparin-binding exosite to the interaction with factor Va in the homologous prothrombinase complex (*43*, *57*). In agreement with this model, addition of inhibitory concentrations of LMWH at subnanomolar protease concentrations accelerates decay of the intrinsic tenase complex (Figure 9). Thus, the binding of heparin oligosaccharide to this exosite disrupts key interactions with the factor VIIIa A2 domain, resulting in antithrombin-independent inhibition of factor X activation by the intrinsic tenase complex.

Intrinsic tenase activity is primarily regulated by instability (loss of the A2 domain) and proteolytic inactivation of factor VIIIa (by factor IXa) (*51*). The factor VIIIa A2 domain directly modulates the catalytic activity of factor IXa, and this effect is enhanced by the A1 domain, markedly increasing the k_{cat} for factor X activation (*58*). The factor VIIIa A3−C1−C2 domain appears to largely account for the observed affinity for factor IXa but completely lacks cofactor activity, suggesting that the factor IXa−A2 domain interaction is the critical surface for modulation of cofactor function (*59*, *60*). Heparin oligosaccharide or mutations in the heparin-binding exosite disrupt the factor IXa−A2 domain interaction, antagonizing and destabilizing cofactor activity within the intrinsic tenase complex. Factor X activation by the intrinsic tenase complex is rate-limiting for thrombin generation by the coagulation cascade, and this critical protease−cofactor interface is likewise limiting for factor X activation by this enzyme complex. These results predict that disruption of the factor IXa−A2 domain interaction will enhance physiologic regulation of intrinsic tenase activity and proportionally reduce thrombin generation, defining a novel molecular target and mechanism for antithrombotic therapy.

ACKNOWLEDGMENT

We thank Darrell Stafford for providing the human factor IX cDNA, wild type, and factor IX R170A cell lines; Andreas Mueller-Beckhaus of the Bayer Corp. for providing recombinant factor VIII (Kogenate FS); and Andre Radloff for assistance with cell culture. Surface plasmon resonance

measurements were performed in the Biophysics Instrumentation Facility at the University of Wisconsin—Madison.

REFERENCES

1. Lawson, J. H., Kalafatis, M., Stram, S., and Mann, K. G. (1994) A model for the tissue factor pathway to thrombin. I. An empirical study, *J. Biol. Chem. 269*, 23357−23366.
2. Rand, M. D., Lock, J. B., van't Veer, C., Gaffney, D. P., and Mann, K. G. (1996) Blood clotting in minimally altered whole blood, *Blood 88*, 3432−3445.
3. van't Veer, C., and Mann, K. G. (1997) Regulation of tissue factor initiated thrombin generation by the stoichiometric inhibitors tissue factor pathway inhibitor, antithrombin-III, and heparin cofactor-II, *J. Biol. Chem. 272*, 4367−4377.
4. van't Veer, C., Golden, N. J., Kalafatis, M., and Mann, K. G. (1997) Inhibitory mechanism of the protein C pathway on tissue factor-induced thrombin generation. Synergistic effect in combination with tissue factor pathway inhibitor, *J. Biol. Chem. 272*, 7983−7994.
5. Hockin, M. F., Jones, K. C., Everse, S. J., and Mann, K. G. (2002) A model for the stoichiometric regulation of blood coagulation, *J. Biol. Chem. 277*, 18322−18333.
6. Lane, D. A., Mannucci, P. M., Bauer, K. A., Bertina, R. M., Bochkov, N. P., Boulyjenkov, V., Chandy, M., Dahlback, B., Ginter, E. K., Miletich, J. P., Rosendaal, F. R., and Seligsohn, U. (1996) Inherited thrombophilia: Part 1, *Thromb. Haemostasis 76*, 651−662.
7. Lane, D. A., Mannucci, P. M., Bauer, K. A., Bertina, R. M., Bochkov, N. P., Boulyjenkov, V., Chandy, M., Dahlback, B., Ginter, E. K., Miletich, J. P., Rosendaal, F. R., and Seligsohn, U. (1996) Inherited thrombophilia: Part 2, *Thromb. Haemostasis 76*, 824−834.
8. Bertina, R. M., Koeleman, B. P., Koster, T., Rosendaal, F. R., Dirven, R. J., de Ronde, H., van der Velden, P. A., and Reitsma, P. H. (1994) Mutation in blood coagulation factor V associated with resistance to activated protein C, *Nature 369*, 64−67.
9. Poort, S. R., Rosendaal, F. R., Reitsma, P. H., and Bertina, R. M. (1996) A common genetic variation in the 3′-untranslated region of the prothrombin gene is associated with elevated plasma prothrombin levels and an increase in venous thrombosis, *Blood 88*, 3698−3703.
10. Koster, T., Blann, A. D., Briet, E., Vandenbroucke, J. P., and Rosendaal, F. R. (1995) Role of clotting factor VIII in effect of von Willebrand factor on occurrence of deep-vein thrombosis, *Lancet 345*, 152−155.
11. van Hylckama Vlieg, A., van der Linden, I. K., Bertina, R. M., and Rosendaal, F. R. (2000) High levels of factor IX increase the risk of venous thrombosis, *Blood 95*, 3678−3682.
12. Meijers, J. C., Tekelenburg, W. L., Bouma, B. N., Bertina, R. M., and Rosendaal, F. R. (2000) High levels of coagulation factor XI as a risk factor for venous thrombosis, *N. Engl. J. Med. 342*, 696−701.
13. Benedict, C. R., Ryan, J., Wolitzky, B., Ramos, R., Gerlach, M., Tijburg, P., and Stern, D. (1991) Active site-blocked factor IXa prevents intravascular thrombus formation in the coronary vasculature without inhibiting extravascular coagulation in a canine thrombosis model, *J. Clin. Invest. 88*, 1760−1765.
14. Choudhri, T. F., Hoh, B. L., Prestigiacomo, C. J., Huang, J., Kim, L. J., Schmidt, A. M., Kisiel, W., Connolly, E. S., Jr., and Pinsky, D. J. (1999) Targeted inhibition of intrinsic coagulation limits cerebral injury in stroke without increasing intracerebral hemorrhage, *J. Exp. Med. 190*, 91−99.
15. Spanier, T. B., Chen, J. M., Oz, M. C., Edwards, N. M., Kisiel, W., Stern, D. M., Rose, E. A., and Schmidt, A. M. (1998) Selective anticoagulation with active site-blocked factor IXA suggests separate roles for intrinsic and extrinsic coagulation pathways in cardiopulmonary bypass, *J. Thorac. Cardiovasc. Surg. 116*, 860−869.
16. Feuerstein, G. Z., Patel, A., Toomey, J. R., Bugelski, P., Nichols, A. J., Church, W. R., Valocik, R., Koster, P., Baker, A., and Blackburn, M. N. (1999) Antithrombotic efficacy of a novel murine antihuman factor IX antibody in rats, *Arterioscler. Thromb. Vasc. Biol. 19*, 2554−2562.
17. Refino, C. J., Jeet, S., DeGuzman, L., Bunting, S., and Kirchhofer, D. (2002) A human antibody that inhibits factor IX/IXa function potently inhibits arterial thrombosis without increasing bleeding, *Arterioscler. Thromb. Vasc. Biol. 22*, 517−522.
18. Hopfner, K. P., Lang, A., Karcher, A., Sichler, K., Kopetzki, E., Brandstetter, H., Huber, R., Bode, W., and Engh, R. A. (1999) Coagulation factor IXa: the relaxed conformation of Tyr99 blocks substrate binding, *Struct. Folding Des. 7*, 989−996.
19. Brandstetter, H., Bauer, M., Huber, R., Lollar, P., and Bode, W. (1995) X-ray structure of clotting factor IXa: active site and module structure related to Xase activity and hemophilia B, *Proc. Natl. Acad. Sci. U.S.A. 92*, 9796−9800.
20. The Columbus Investigators (1997) Low-molecular-weight heparin in the treatment of patients with venous thromboembolism, *N. Engl. J. Med. 337*, 657−662.
21. Koopman, M. M., Prandoni, P., Piovella, F., Ockelford, P. A., Brandjes, D. P., van der Meer, J., Gallus, A. S., Simonneau, G., Chesterman, C. H., and Prins, M. H. (1996) Treatment of venous thrombosis with intravenous unfractionated heparin administered in the hospital as compared with subcutaneous low-molecular-weight heparin administered at home, *N. Engl. J. Med. 334*, 682−687.
22. Levine, M., Gent, M., Hirsh, J., Leclerc, J., Anderson, D., Weitz, J., Ginsberg, J., Turpie, A. G., Demers, C., and Kovacs, M. (1996) A comparison of low-molecular-weight heparin administered primarily at home with unfractionated heparin administered in the hospital for proximal deep-vein thrombosis, *N. Engl. J. Med. 334*, 677−681.
23. Bedsted, T., Swanson, R., Chuang, Y. J., Bock, P. E., Bjork, I., and Olson, S. T. (2003) Heparin and calcium ions dramatically enhance antithrombin reactivity with factor IXa by generating new interaction exosites, *Biochemistry 42*, 8143−8152.
24. Izaguirre, G., Zhang, W., Swanson, R., Bedsted, T., and Olson, S. T. (2003) Localization of an antithrombin exosite that promotes rapid inhibition of factors Xa and IXa dependent on heparin activation of the serpin, *J. Biol. Chem. 278*, 51433−51440.
25. Miletich, J. P., Jackson, C. M., and Majerus, P. W. (1978) Properties of the factor Xa binding site on human platelets, *J. Biol. Chem. 253*, 6908−6916.
26. Rezaie, A. R. (2001) Prothrombin protects factor Xa in the prothrombinase complex from inhibition by the heparin-antithrombin complex, *Blood 97*, 2308−2313.
27. Barrow, R. T., Parker, E. T., Krishnaswamy, S., and Lollar, P. (1994) Inhibition by heparin of the human blood coagulation intrinsic pathway factor X activator, *J. Biol. Chem. 269*, 26796−26800.
28. Gray, E., Cesmeli, S., Lormeau, J. C., Davies, A. B., and Lane, D. A. (1994) Low affinity heparin is an antithrombotic agent, *Thromb. Haemostasis 71*, 203−207.
29. Sheehan, J., and Lan, H. (1998) Phosphorothioate oligonucleotides inhibit the intrinsic tenase complex, *Blood 92*, 1617−1625.
30. Sheehan, J. P., and Phan, T. M. (2001) Phosphorothioate oligonucleotides inhibit the intrinsic tenase complex by an allosteric mechanism, *Biochemistry 40*, 4980−4989.
31. Sheehan, J. P., Kobbervig, C. E., and Kirkpatrick, H. M. (2003) Heparin inhibits the intrinsic tenase complex by interacting with an exosite on factor IXa, *Biochemistry 42*, 11316−11325.
32. MacDonald, R. C., MacDonald, R. I., Menco, B. P., Takeshita, K., Subbarao, N. K., and Hu, L. R. (1991) Small-volume extrusion apparatus for preparation of large, unilamellar vesicles, *Biochim. Biophys. Acta 1061*, 297−303.
33. Chen, P., Toribara, T., and Warner, H. (1956) *Anal. Chem. 28*, 1756−1758.
34. Chang, J., Jin, J., Lollar, P., Bode, W., Brandstetter, H., Hamaguchi, N., Straight, D. L., and Stafford, D. W. (1998) Changing residue 338 in human factor IX from arginine to alanine causes an increase in catalytic activity, *J. Biol. Chem. 273*, 12089−12094.
35. Southern, P. J., and Berg, P. (1982) Transformation of mammalian cells to antibiotic resistance with a bacterial gene under control of the SV40 early region promoter, *J. Mol. Appl. Genet. 1*, 327−341.
36. Yan, S. C., Razzano, P., Chao, Y. B., Walls, J. D., Berg, D. T., McClure, D. B., and Grinnell, B. W. (1990) Characterization and novel purification of recombinant human protein C from three mammalian cell lines, *Biotechnology (New York) 8*, 655−661.
37. Cote, H. C., Stevens, W. K., Bajzar, L., Banfield, D. K., Nesheim, M. E., and MacGillivray, R. T. (1994) Characterization of a stable form of human meizothrombin derived from recombinant prothrombin (R155A, R271A, and R284A), *J. Biol. Chem. 269*, 11374−11380.
38. Lozier, J. N., Monroe, D. M., Stanfield-Oakley, S., Lin, S. W., Smith, K. J., Roberts, H. R., and High, K. A. (1990) Factor IX

New London: substitution of proline for glutamine at position 50 causes severe hemophilia B, *Blood 75*, 1097−1104.
39. Myszka, D. G. (2000) Kinetic, equilibrium, and thermodynamic analysis of macromolecular interactions with BIACORE, *Methods Enzymol. 323*, 325−340.
40. Limbird, L. (1995) *Cell Surface Receptors: A Short Course on Theory and Methods*, Kluwer Academic Publishers, Boston, MA.
41. Segel, I. H. (1975) *Enzyme Kinetics: Behavior and Analysis of Rapid Equilibrium and Steady-State Enzyme Systems*, John Wiley and Sons, New York.
42. Dixon, M., and Webb, E. (1979) *Enzymes*, Academic Press, New York.
43. Rezaie, A. R. (2000) Identification of basic residues in the heparin-binding exosite of factor Xa critical for heparin and factor Va binding, *J. Biol. Chem. 275*, 3320−3327.
44. Sheehan, J. P., and Sadler, J. E. (1994) Molecular mapping of the heparin-binding exosite of thrombin, *Proc. Natl. Acad. Sci. U.S.A. 91*, 5518−5522.
45. Sturzebecher, J., Kopetzki, E., Bode, W., and Hopfner, K. P. (1997) Dramatic enhancement of the catalytic activity of coagulation factor IXa by alcohols, *FEBS Lett. 412*, 295−300.
46. Mathur, A., and Bajaj, S. P. (1999) Protease and EGF1 domains of factor IXa play distinct roles in binding to factor VIIIa. Importance of helix 330 (helix 162 in chymotrypsin) of protease domain of factor IXa in its interaction with factor VIIIa, *J. Biol. Chem. 274*, 18477−18486.
47. Kolkman, J. A., Lenting, P. J., and Mertens, K. (1999) Regions 301−303 and 333−339 in the catalytic domain of blood coagulation factor IX are factor VIII-interactive sites involved in stimulation of enzyme activity, *Biochem. J. 339*, 217−221.
48. Bajaj, S. P., Schmidt, A. E., Mathur, A., Padmanabhan, K., Zhong, D., Mastri, M., and Fay, P. J. (2001) Factor IXa:factor VIIIa interaction. helix 330−338 of factor ixa interacts with residues 558−565 and spatially adjacent regions of the a2 subunit of factor VIIIa, *J. Biol. Chem. 276*, 16302−16309.
49. Lollar, P., and Parker, C. G. (1990) pH-dependent denaturation of thrombin-activated porcine factor VIII, *J. Biol. Chem. 265*, 1688−1692.
50. Lollar, P., Knutson, G. J., and Fass, D. N. (1984) Stabilization of thrombin-activated porcine factor VIII:C by factor IXa phospholipid, *Blood 63*, 1303−1308.
51. Fay, P. J., Beattie, T. L., Regans, L. M. O., Brien, L. M., and Kaufman, R. J. (1996) Model for the factor VIIIa-dependent decay of the intrinsic factor Xase. Role of subunit dissociation and factor IXa-catalyzed proteolysis, *J. Biol. Chem. 271*, 6027−6032.
52. Green, P. M., Giannelli, F., Sommer, S. S., Poon, M.-C., Ludwig, M., Schwaab, R., Rietsma, P. H., Goossens, M., Yoshioka, A., Figueriredo, M. S., Tagariello, G., and Brownlee, G. G. (2003) Haemophilia B Mutation Database (www.kcl.ac.uk/ip/petergreen/haemBdatabase.html).
53. Jenkins, P. V., Dill, J. L., Zhou, Q., and Fay, P. J. (2004) Clustered basic residues within segment 484−510 of the factor VIIIa A2 subunit contribute to the catalytic efficiency for factor Xa generation, *J. Thromb. Haemostasis 2*, 452−458.
54. Walker, R. K., and Krishnaswamy, S. (1994) The activation of prothrombin by the prothrombinase complex. The contribution of the substrate-membrane interaction to catalysis, *J. Biol. Chem. 269*, 27441−27450.
55. Krishnaswamy, S., Field, K. A., Edgington, T. S., Morrissey, J. H., and Mann, K. G. (1992) Role of the membrane surface in the activation of human coagulation factor X, *J. Biol. Chem. 267*, 26110−26120.
56. Yang, L., Manithody, C., and Rezaie, A. R. (2002) Localization of the heparin binding exosite of factor IXa, *J. Biol. Chem. 277*, 50756−50760.
57. Rudolph, A. E., Porche-Sorbet, R., and Miletich, J. P. (2001) Definition of a factor Va binding site in factor Xa, *J. Biol. Chem. 276*, 5123−5128.
58. Fay, P. J., Koshibu, K., and Mastri, M. (1999) The A1 and A2 subunits of factor VIIIa synergistically stimulate factor IXa catalytic activity, *J. Biol. Chem. 274*, 15401−15406.
59. Lenting, P. J., Donath, M. J., van Mourik, J. A., and Mertens, K. (1994) Identification of a binding site for blood coagulation factor IXa on the light chain of human factor VIII, *J. Biol. Chem. 269*, 7150−7155.
60. Fay, P. J., and Koshibu, K. (1998) The A2 subunit of factor VIIIa modulates the active site of factor IXa, *J. Biol. Chem. 273*, 19049−19054.

BI047934A